(Received 16 April 2025, Accepted 14 May 2025, Scheduled 16 June 2025)

Flat-Plate Dipole Antenna for Wi-Fi 8 and 6G Operation

Saou-Wen Su*, Tung-Chan Yu, and Ju-Cheng Huang

Department of Computer and Communication Engineering
National Kaohsiung University of Science and Technology, Kaohsiung 824, Taiwan

ABSTRACT: A planar, short-circuited dipole design, constructed from cutting a flat metallic plate, capable of operating in the 2.4/5/6 GHz Wi-Fi 8 bands and also the 6G upper mid-band in the 7125–8400 MHz range is presented. The antenna comprises two folded dipole arms, each of which has a cut-out portion, with one short-circuiting portion connecting them. The plate dipole can operate at its 0.5-, 1.5-, and 2.5-λ resonant modes with two higher-order resonances forming a very wide 10-dB impedance bandwidth of about 5.0–9.4 GHz, easily covering the 5150–8400 MHz band for the 5/6 GHz Wi-Fi bands and 6G upper mid-band. The design is simple in structure, has a compact size of 10 mm $\times$ 30 mm (0.08-λ $\times$ 0.24-λ at 2.4 GHz), and also shows good radiation performance. The design concept is elucidated and discussed in this paper with the numerical and experimental results.

1. INTRODUCTION

Dipole antennas are one of the fundamental antennas theoretically analyzed [1]. For years, many dipole designs focusing on multiband and wideband operation have been reported [2–8], including modifying feeding to combine 0.5- and 1.0-λ dipole modes [2–4], loading dipole arms with slots or slits to increase multiple resonant paths [5, 6], and using inherent harmonic modes [7, 8]. Many of these works are either bulky or intricate in structure. In this paper, a simple flat-plate dipole is introduced that has multiband and wideband characteristics for Wi-Fi 8 (IEEE 802.11bn) operation [9] and also the new 6G upper mid-band in the 7125–8400 MHz range [10, 11]. Wi-Fi 8 is expected to be approved in 2028, with early certifications projected before 2027. Additionally, the commercialization of 6G networks is anticipated around 2030. Accordingly, the antennas that work for wireless heterogeneous networks [12, 13], such as Wi-Fi 8 and 6G communications, are expected to arrive shortly. The dipole size is compact with the dimensions 10 mm $\times$ 30 mm (0.08-λ $\times$ 0.24-λ at 2.4 GHz in free space) and can be manufactured by cutting a flat metallic plate in mass production. The lower band of the design at the 0.5-λ dipole mode can operate in the 2.4 GHz (2400–2484 MHz) Wi-Fi band, while the upper bands formed by the 1.5- and 2.5-λ modes produce a wide 10-dB return-loss bandwidth about 5.0–9.4 GHz, easily covering the 5/6 GHz (5150–7125 MHz) Wi-Fi bands and 6G upper mid-band. The design is fed by the mini-coaxial cable and is not required to be integrated with the system ground plane, allowing engineers to have much freedom to locate the antenna within the devices for better transceiving performance. The details of the antenna design are elucidated in the article.

2. SHORT-CIRCUITED FLAT-PLATE DIPOLE

2.1. Dipole Configuration

Figure 1 shows the geometry of the proposed flat-plate dipole antenna. The design primarily comprises two symmetrical folded arms and a short-circuiting portion that connects the two arms. Each radiating dipole arm is loaded with a cut-out portion of length L and width W. The antenna frequencies of the first (0.5-λ) and second (1.5-λ) dipole resonances can be adjusted by the dimensions of the cut-out portion. Related parametric studies are presented in the following section. Additionally, the short-circuiting portion contributes to better antenna matching and makes a one-piece plate-dipole structure possible, as previously studied in [14, 15]. In this work, the dipole can produce three resonances that correspond to its 0.5-, 1.5-, and 2.5-λ harmonic modes at about 2.45, 5.41, and 8.47 GHz. The two upper bands attributed to the 1.5- and 2.5-λ modes are combined to form a very wide 10-dB impedance bandwidth (about 4.4 GHz). This bandwidth easily includes the 5/6 GHz Wi-Fi bands and the 7125–8400 MHz range of the 6G upper mid-band.

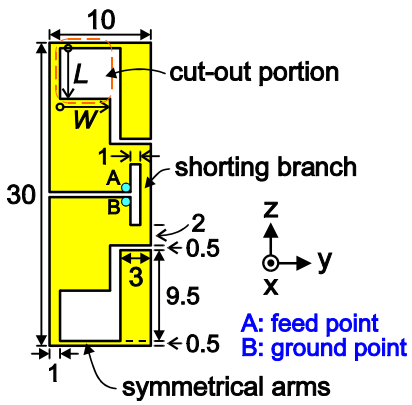

FIGURE 1. Geometry of the short-circuited plate-dipole antenna.

* Corresponding author: Saou-Wen Su (SaouWenSu@nkust.edu.tw).

The one-piece dipole without separate radiating arms can be made by cutting a single metallic plate of 0.2-mm stainless-steel sheet. The rectangle size of the design measures 10 mm $\times$ 30 mm. This compact structure makes the design suitable for internal antenna applications for communication devices, such as consumer premise equipment (CPE). For industrial applications, the proposed dipole is fed by a 50-Ω mini-coaxial cable with inner signal wires soldered at point A and the outer grounding sheath at point B. The miniature connector of the coaxial cable will be mounted on the wireless module within the devices. A diminutive feed gap of 0.5 mm between points A and B is set in this study, working together with the shorting branch for antenna matching [14, 15]. A photo of a fabricated prototype is shown in Fig. 2. To achieve more stable return-loss curves, a 70-mm-long, RG405 semi-rigid coaxial cable was utilized in the experiments to test the proposed dipole. The RG405 semi-rigid coaxial cable can operate up to 40 GHz, and per 1 meter long, the loss at 2 GHz is about 0.99 dB and at 5 GHz is about 0.16 dB. That is, the cable loss is very low. Several antenna parameters have been analyzed using an electromagnetic (EM) simulator, Ansys High Frequency Structure Simulator (HFSS) [16] that primarily uses the finite element method, to achieve maximum achievable bandwidth. The following subsection presents a discussion of some selected results.

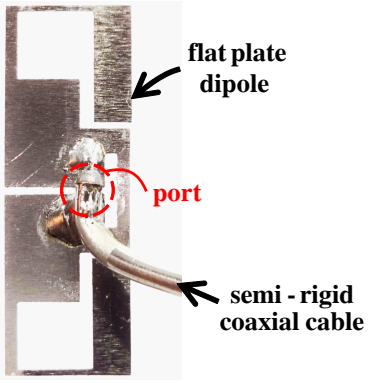

FIGURE 2. Photo of a fabricated prototype; $L = 5$ mm, $W = 5$ mm.

2.2. Parametric Analyses

Figure 3 shows the return losses of the proposed design and reference dipole, similar but different in size compared with the dipole in [14]. The proposed dipole covers all the 2.4/5/6 GHz Wi-Fi 8 bands and the 6G upper-mid band in the 7125-8400 MHz range with good impedance matching surpassing 10 dB return loss. Three resonant modes at about 2.45, 5.41, and 8.47 GHz are also observed. For the reference case (the dipole without the cut-out portions, see inset in Fig. 3), the achievable lower-band resonance with the same 0.5-λ dipole mode moves from 2.45 to 3.19 GHz. That is, to achieve the same lower-band frequencies, the length of the reference dipole needs to increase by about 1.3 times (about 38–39 mm long) of the proposed plate dipole. Accordingly, the proposed design reaches an overall 23% size reduction, compared with the size of the reference case. In addition, the lower-edge frequency (f_L) of the two upper bands for the reference dipole is also shifted from 5 to 5.85 GHz, which

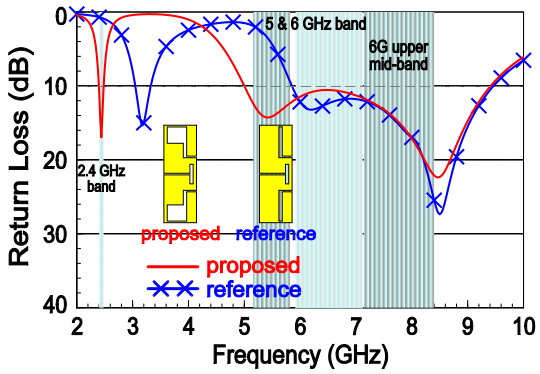

FIGURE 3. Return losses for the proposed ($L = 5$ mm) and reference ($L = 0$ mm) dipoles.

cannot meet the desired specification. Finally, it is noteworthy that the upper-edge frequencies (f_U) for both the proposed and reference cases are quite similar, around 9.41–9.46 GHz.

The associated surface currents for the proposed dipole are presented in Fig. 4. 2.45, 5.41, and 8.47 GHz are sampled frequencies representing the three most matched antenna frequencies as shown in Fig. 3. At 2.45 GHz in the 2.4 GHz band, the strong in-phase currents are evenly distributed along the 0.5-λ dipole arms from the end to the opposite end of the dipole. At 5.41 GHz, two nulls are identified at the corners of the cut-out portions of the dipole, reflecting the 1.5-λ dipole mode. As for the frequency at 8.47 GHz, four nulls are observed along the current path, which represents the 2.5-λ dipole mode.

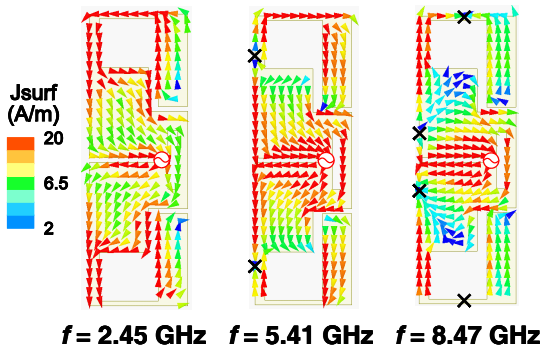

FIGURE 4. Surface current distributions at 2.45, 5.41, and 8.47 GHz.

The studies on the selected dipole parameters are elucidated in Fig. 5. All the dimensions are kept the same as those shown in Fig. 1. Only one antenna parameter is varied at a time in the analyses. Fig. 5(a) gives the return losses as a function of the cut-out portion length L. This parameter significantly affects the frequency ratio between the 1.5- and 0.5-λ dipole modes. As the length L increases, the frequency ratio increases, too. When L is equal to 5 mm (the preferred value in this study), the frequency ratio (5.42 to 2.44 GHz) is about 2.22. The effects of the width W of the cut-out portion are shown in Fig. 5(b). This width W primarily controls the frequencies of the 1.5-λ dipole mode. With increasing width, the occurrence of the 1.5-λ mode is shifted toward the lower frequencies, due to an increased effective resonant length around the current-null region. Finally, in Fig. 5(c), the effects of the strip width T on the return losses

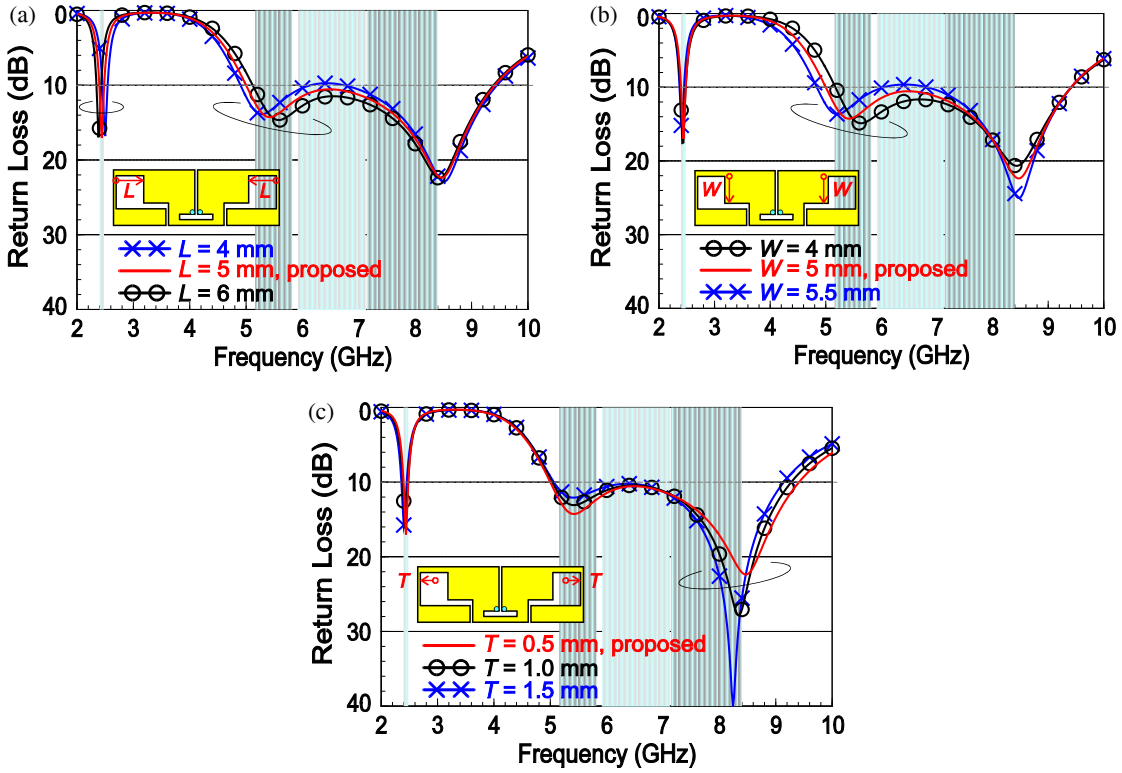

FIGURE 5. Return losses as a function of (a) length L and (b) width W of the cut-out portion and (c) the extended strip width T; other dimensions remain the same as shown in Fig. 1.

are relatively seen at the 2.5-λ dipole mode around 8.4 GHz. Note that the width T analyzed in this case was extended outwards, which increases the total antenna length (see the inset in the same figure). The effects are primarily because the current nulls of the 2.5-λ dipole resonance are present on the thin sections, as seen in Fig. 4 of surface currents.

3. EXPERIMENTAL VERIFICATION

The simulated and measured return losses for the proposed dipole and fabricated prototype are shown in Fig. 6. The experimental results agree well with the simulated data, based on the finite element method of the EM simulator. Three resonant modes around 2.45, 5.41, and 8.47 GHz can be spotted with good impedance surpassing 10 dB return loss. The two upper bands cover about 4 GHz 10-dB impedance bandwidth.

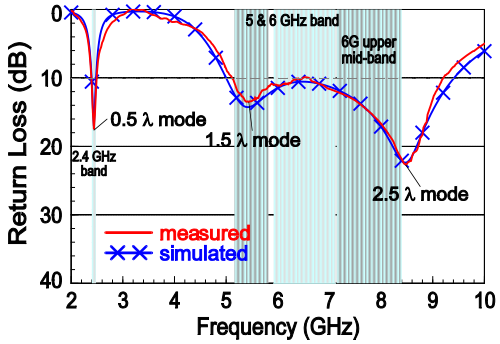

FIGURE 6. Simulated and measured return losses for the proposed prototype.

The proposed design effectively covers the whole 2.4/5/6 GHz Wi-Fi 8 bands and the 7125–8400 MHz range of the 6G upper mid-band.

Figure 7 plots the normalized 2-D radiation patterns at 2.45, 5.41, and 8.47 GHz in the E-total field. The simulated results are presented in circle lines. The measured results, in general, correspond well with the simulation. The E-total fields are chosen here in lieu of separate E_θ and E_ϕ fields because, from previous throughput measurements in the industry, a significant correlation was established between the actual data rate (throughput values) and E-total patterns. Overall, omnidirectional radiation patterns in the x-y planes are achieved for all bands, highlighting the radiating nature of the dipole antenna. Relatively weaker radiation intensity along the z-axis is noticeable in the 0.5-λ dipole mode of the lower band but less apparent in the two upper bands due to the bending dipole arms and in-phase current flow.

Figure 8 displays the measured realized antenna gain (E-total) and total efficiency [17]. The simulation plotted in blue cross lines generally coincides with the measurement. The lossless radiation efficiency (e) is the ratio of the antenna's total radiated power over the spherical region to its input power of 1 mWatt in the measurements. The total efficiency is obtained from the radiation efficiency (e) multiplied by a factor of the mismatch element $(1 - |\Gamma|^2)$ (Γ represents the reflection). Hence, the measurements account for signal degradation from cable losses and antenna impedance mismatch. The proposed dipole was measured in an anechoic chamber following the great circle method described by the Cellular Telecommunica-

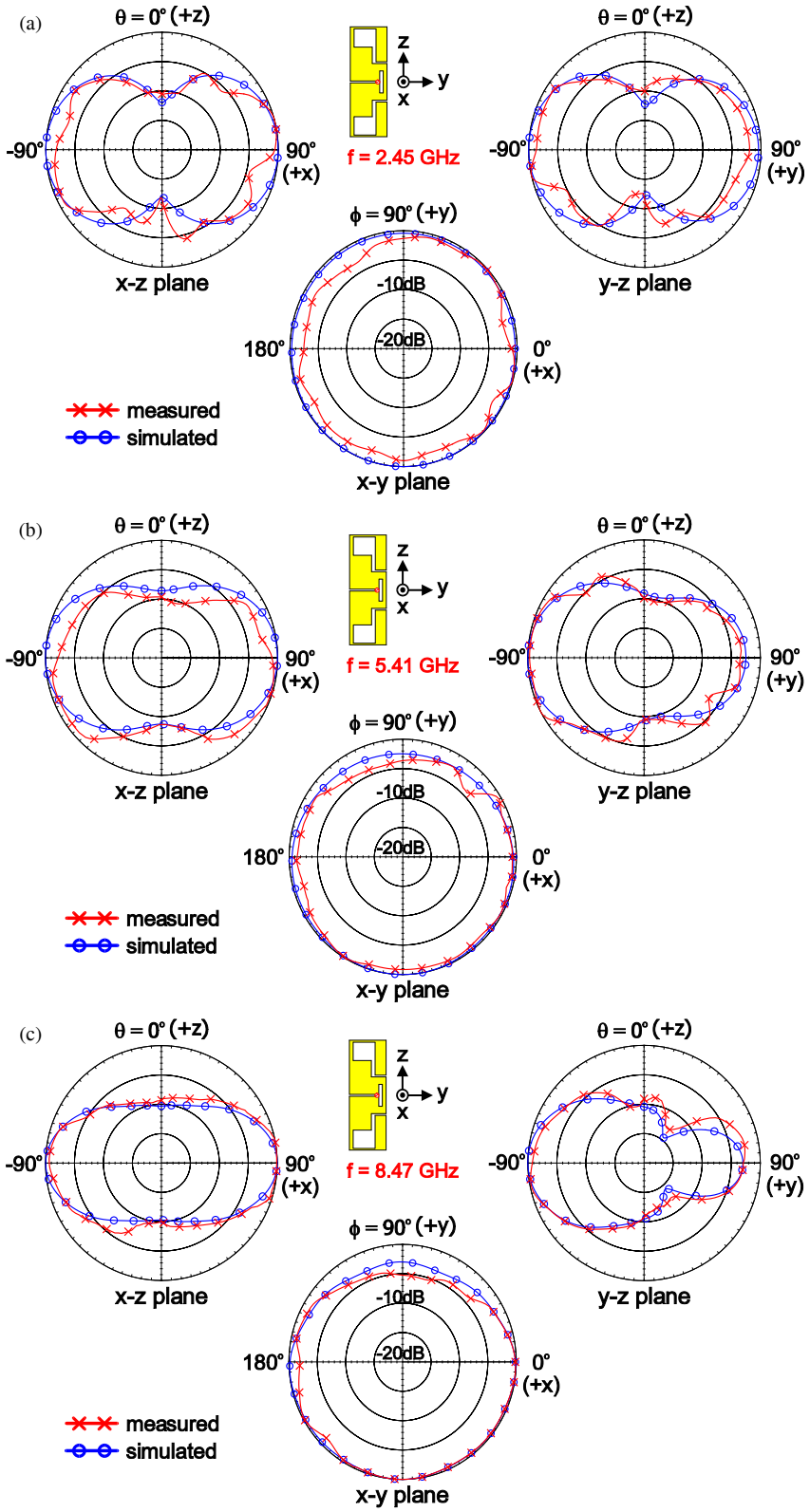

FIGURE 7. Simulated and measured 2-D radiation patterns at (a) 2.45, (b) 5.41, and (c) 8.47 GHz.

tions and Internet Association (CTIA) industrial standard [18]. A 5-degree step in both theta and phi directions was taken over the spherical region. The realized gain in the 2.4 GHz band is 2.1–2.5 dBi with a stable total efficiency of around 78%. For the 5/6 GHz bands, the gain is 3.3–4.1 dBi, with the total efficiency larger than 78%. As for the 6G upper-mid band in the 7125–8400 MHz range, the gain is 3.4–4.4 dBi, with the efficiency around 81–85%.

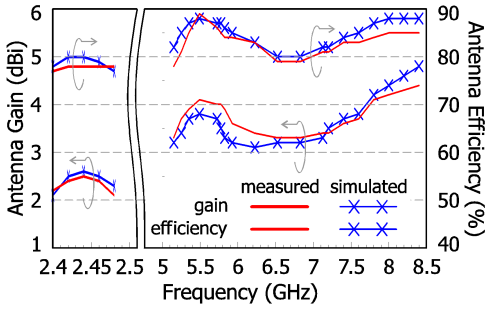

FIGURE 8. Measured realized gain and total efficiency in the 2.4/5/6 GHz bands and 6G upper mid-band.

4. CONCLUSION

A multiband and wideband plate dipole, made of a one-piece stainless-steel plate, for Wi-Fi 8 and 6G upper mid-band operation is proposed in this paper. The design can produce three resonances at the respective 0.5-, 1.5-, and 2.5-λ dipole modes. The two upper bands at the 1.5- and 2.5-λ modes are combined to form a very wide 10-dB impedance bandwidth (about 4.4 GHz), such that the 5150–8400 MHz range is easily covered for the 5/6 GHz Wi-Fi bands and 6G upper mid-band. The frequencies of each band can be fine-adjusted through parametric evaluation. The proposed dipole has a compact form factor and can provide good radiation properties. The result of the total efficiency for the 2.4 GHz Wi-Fi band is around 78%, while that in the two upper bands in 5150–8400 MHz reaches about 78%–85%. The proposed design is promising for Wi-Fi 8 and 6G heterogeneous communications in the near future.

REFERENCES

[1] Kraus, J. D. and R. J. Marhefka, *Antennas for All Applications*, 165–176, McGraw-Hill, Chap. 6, 2003.

[2] Chi, Y.-W., K.-L. Wong, and S.-W. Su, "Broadband printed dipole antenna with a step-shaped feed gap for DTV signal reception," *IEEE Transactions on Antennas and Propagation*, Vol. 55, No. 11, 3353–3356, 2007.

[3] Su, S.-W. and F.-S. Chang, "Wideband rod-dipole antenna with a modified feed for DTV signal reception," *Progress In Electromagnetics Research Letters*, Vol. 12, 127–132, 2009.

[4] Huang, H., B. Li, X. Li, and Y. Liu, "A wideband dipole based on odd and even mode fusion," *IEEE Antennas and Wireless Propagation Letters*, Vol. 23, No. 2, 783–787, 2024.

[5] Su, C.-M., H.-T. Chen, and K.-L. Wong, "Printed dual-band dipole antenna with U-slotted arms for 2.4/5.2 GHz WLAN operation," *Electronics Letters*, Vol. 38, No. 22, 1308–1309, 2002.

[6] Nguyen, V.-A., B.-Y. Park, S.-O. Park, and G. Yoon, "A planar dipole for multiband antenna systems with self-balanced impedance," *IEEE Antennas and Wireless Propagation Letters*, Vol. 13, 1632–1635, 2014.

[7] Xiao, B., H. Wong, M. Li, B. Wang, and K. L. Yeung, "Dipole antenna with both odd and even modes excited and tuned," *IEEE Transactions on Antennas and Propagation*, Vol. 70, No. 3, 1643–1652, 2022.

[8] You, J. and Y. Dong, "Pattern reconfigurable dipole antenna based on odd and even mode principle for 5G-NR communications," *IEEE Transactions on Antennas and Propagation*, Vol. 72, No. 10, 8028–8033, 2024.

[9] Galati-Giordano, L., G. Geraci, M. Carrascosa, and B. Bellalta, "What will Wi-Fi 8 be? A primer on IEEE 802.11 bn ultra high reliability," *IEEE Communications Magazine*, Vol. 62, No. 8, 126–132, 2024.

[10] WRC-23 (World Radiocommunication Conference 2023), "Final Acts of the WRC-23", https://www.itu.int/wrc-23/documents/.

[11] Americas, G., "The 6G upgrade in the 7-8 GHz spectrum range: Coverage capacity and technology," https://www.5gamericas.org/wp-content/uploads/2024/10/The-6G-Upgrade-in-the-7-8-GHz-Spectrum-Id.pdf.

[12] Lee, C.-T., C.-C. Wan, and S.-W. Su, "Multi-laptop-antenna designs for 2.4/5/6 GHz WLAN and 5G NR77/78/79 operation," in *2020 International Symposium on Antennas and Propagation (ISAP)*, 421–422, Osaka, Japan, 2021.

[13] Yusuf, D. P., F.-H. Chu, and S.-W. Su, "Ultra-wideband Wi-Fi 6E/5G NR antenna for laptop applications," in *2022 Asia-Pacific Microwave Conference (APMC)*, 548–550, Yokohama, Japan, 2022.

[14] Su, S.-W. and J.-H. Chou, "Compact coaxial-line-fed flat-plate dipole antenna for WLAN applications," *Microwave and Optical Technology Letters*, Vol. 50, No. 2, 420–422, 2008.

[15] Su, S.-W. and T.-C. Hong, "A bent, short-circuited, metal-plate dipole antenna for 2.4-GHz WLAN operation," *Progress In Electromagnetics Research Letters*, Vol. 16, 191–197, 2010.

[16] Ansys HFSS, Ansys Inc., https://www.ansys.com/en-gb/products/electronics/ansys-hfss.

[17] Balanis, C. A., *Antenna Theory: Analysis and Design*, John Wiley & Sons, 2016.

[18] CTIA, the Wireless Association, https://ctiacertification.org/program/over-the-air-performance-testing/.